Modulated amplitude waves in Bose-Einstein condensates

Mason A. Porter*
School of Mathematics and Center for Nonlinear Science, Georgia Institute of Technology, Atlanta, Georgia 30332, USA

Predrag Cvitanović
Center for Nonlinear Science and School of Physics, Georgia Institute of Technology, Atlanta, Georgia 30332, USA
(Received 30 October 2003; published 12 April 2004)

We analyze spatiotemporal structures in the Gross-Pitaevskii equation to study the dynamics of quasi-one-dimensional Bose-Einstein condensates (BECs) with mean-field interactions. A coherent structure ansatz yields a parametrically forced nonlinear oscillator, to which we apply Lindstedt's method and multiple-scale perturbation theory to determine the dependence of the intensity of periodic orbits ("modulated amplitude waves") on their wave number. We explore BEC band structure in detail using Hamiltonian perturbation theory and supporting numerical simulations.

DOI: 10.1103/PhysRevE.69.047201 PACS number(s): 05.45.Ac, 03.75.Lm, 05.30.Jp

At low temperatures, particles in a gas can reside in the same quantum (ground) state, forming a Bose-Einstein condensate [1–6]. When considering only two-body, mean-field interactions, the condensate wave function ψ satisfies the Gross-Pitaevskii (GP) equation, a cubic nonlinear Schrödinger equation (NLS) with an external potential

$$i\hbar\psi_t = -[\hbar^2/(2m)]\psi_{xx} + g|\psi|^2\psi + V(x)\psi, \tag{1}$$

where m is the mass of a gas particle, $V(x)$ is an external potential, $g=[4\pi\hbar^2 a/m][1+O(\iota^2)]$, a is the (two-body) s-wave scattering length, and $\iota=\sqrt{|\psi|^2|a|^3}$ is the dilute gas parameter [2,7]. The quantity a is determined by the atomic species in the condensate. Interactions between atoms are repulsive when $a>0$ and attractive when $a<0$. When $a\approx 0$, one is in the ideal gas regime.

The quasi-one-dimensional (quasi-1D) regime employed in Eq. (1) is suitable when the transverse dimensions of the condensate are on the order of its healing length and its longitudinal dimension is much larger than its transverse ones [2,8–10]. In this situation, one employs the 1D limit of a 3D mean-field theory rather than a true 1D mean-field theory, as would be appropriate were the tranverse dimension on the order of the atomic interaction length or the atomic size.

In this paper, we examine uniformly propagating coherent structures by applying the ansatz $\psi(x-vt,t)=R(x-vt)\exp(i[\theta(x-vt)-\omega t])$, where $R\equiv|\psi|$ is the magnitude (intensity) of the wave function, v is the velocity of the coherent structure, $\theta(x)$ determines its phase, and ω is the temporal frequency (chemical potential). Considering a coordinate system that travels with speed v (by defining $x'=x-vt$ and relabeling x' as x) yields

$$\psi(x,t)=R(x)\exp\{i[\theta(x)-\omega t]\}. \tag{2}$$

[From a physical perspective, we consider the case $v=0$, as $v(x')=V(x-vt)$.] When the (temporally periodic) coherent structure (2) is also spatially periodic, it is called a *modulated amplitude wave* (MAW). The orbital stability of coherent structures (2) for the GP with elliptic potentials has been studied by Bronski and co-authors [8–10]. To obtain information about sinusoidal potentials, one takes the limit as the elliptic modulus k approaches zero [11,12]. When $V(x)$ is periodic, the resulting MAWs generalize the Bloch modes that occur in linear systems with periodic potentials, as one is considering a nonlinear Floquet-Bloch theory rather than a linear one [13–17].

In this paper, we employ phase space methods and Hamiltonian perturbation theory to examine the band structure of such MAWs. Prior work in this area has utilized numerical simulations [15–17].

The uniqueness of our work lies in its illumination of BEC band structure through the use of perturbation theory and supporting numerical simulations to examine $2n$:1 spatial subharmonic resonances in BECs in period lattices. Such resonances correspond to spatially periodic solutions of period $2n$ and generalize the "period doubled" states (in $|\psi|^2$) studied by Machholm *et al.* [18], which pertain to the experimental observations of Cataliotti *et al.* [19].

Inserting Eq. (2) into the GP (1), equating real and imaginary parts, and simplifying yields

$$R' = S,$$

$$S' = \frac{c^2}{R^3} - \frac{2m\omega R}{\hbar} + \frac{2mg}{\hbar^2}R^3 + \frac{2m}{\hbar^2}V(x)R. \tag{3}$$

The parameter c is defined via the relation $\theta'(x)=c/R^2$, which is an expression of conservation of angular momentum [8]. Null angular momentum solutions, which constitute an important special case, satisfy $c=0$.

When $V(x)\equiv 0$, the 2D dynamical system (3) is autonomous and hence integrable. Its equilibria and the stability thereof are discussed in detail in Ref. [21]. When $g>0$, $\omega>0$, and $c=0$, which is the primary case for which we study the band structure, one obtains a neutrally stable equilibrium (a center) at $(R,S)=(0,0)$ and unstable equilibria (saddles) at $(\pm\sqrt{\hbar\omega/g},0)$; see Fig. 1.

*Email address: mason@math.gatech.edu
URL: www.math.gatech.edu/~ mason

 ©2004 The American Physical Society

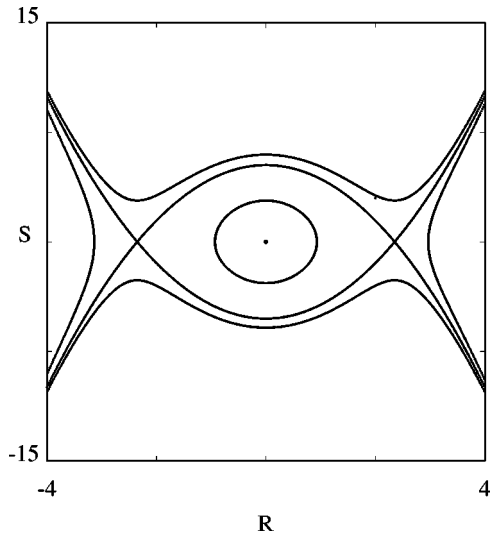

FIG. 1. Phase portrait of a repulsive BEC with no external potential and $\omega=10$. In this plot, the two-body scattering length is $a=0.072$ nm, obtained for atomic hydrogen (^{1}H) [20]. Orbits inside the separatrix have bounded intensity $R(x)$ with increasing period as one approaches the separatrix. The variables R and $S=R'$ are scaled quantities obtained with $m=1/2$ and $\hbar=1$.

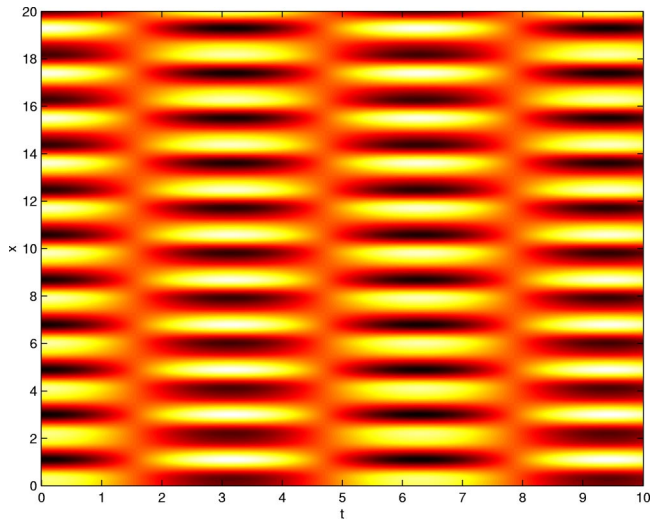

FIG. 2. An example of a spatially quasiperiodic coherent structure for ^1H in a sinusoidal lattice. As in Fig. 1, $\omega=10$, $a=0.072$, $c=0$, $m=1/2$, and $\hbar=1$. Additionally, $V_0=10$. This plot, which was obtained from the coherent structure ansatz, depicts Re(ψ), with the initial point $(R(0),S(0))=(0.05,0.05)$ inside the separatrix in Fig. 1. The darkest portions are the most negative, and the lightest are the most positive. The quantities R and S are defined as in Fig. 1.

We employed Lindstedt's method to study the dependence of the wave number of periodic orbits (centered at the origin) of Eq. (3) on the intensity R when $V(x)\equiv 0$ [13]. We assumed $g=\varepsilon\overline{g}$, where $\varepsilon\ll 1$ and $\overline{g}=O(1)$. The wave number is then $\alpha=1-3gA^2/(8\omega\hbar)+O(\varepsilon^2)$, where $R(\xi)=R_0(\xi)+O(\varepsilon)$, $\xi:=\alpha x$, $R_0(\xi)=A\cos(\beta\xi)$, and $\beta:=\sqrt{2m\omega/\hbar}$.

To study the wave number-intensity relations of periodic orbits in the presence of external potentials, we expand the spatial variable x in multiple scales. We define "stretched space" $\xi:=\alpha x$ as in the integrable situation and "slow space" $\eta:=\varepsilon x$. We consider potentials of the form $V(x)=\varepsilon\overline{V}(\xi,\eta)$, where $\overline{V}(\xi,\eta)=\overline{V}_0\sin[\kappa(\xi-\xi_0)]+\overline{V}_1(\eta)$ and $\overline{V}_1(\eta)$, which is of order $O(1)$, is arbitrary but slowly varying. Cases of particular interest include $\overline{V}_1(\eta)=0$ (periodic potential) and $\overline{V}_1(\eta)=\overline{V}_h(\eta-\eta_0)^2$ (superposition of periodic and harmonic potentials). When $\overline{V}_h\ll\overline{V}_0$, this latter potential is dominated by its periodic contribution for many periods [22,23]. The wave number parameter is $\kappa=2\pi/T$, where T represents the periodicity of the underlying lattice. Optical lattices with more than 20 periods have now been created experimentally [24]. Spatially periodic potentials, which is the primary case we consider, have been employed in experimental studies of BECs [25,26]. They have also been studied theoretically in Refs. [8–10,16,17,22,23,27]. An example of a coherent structure for hydrogen in the presence of a periodic lattice is depicted in Fig. 2. Coherent structures in other situations, such as for ^{85}Rb (for which $a=-0.9$), are examined in Ref. [21].

When $\kappa\neq\pm 2\beta$, the wave number-intensity relation for periodic orbits of Eq. (3) is

$$\alpha(C)=1-\frac{3g}{8\omega\hbar}C^2-\frac{1}{2\omega\hbar}V_1(x)+O(\varepsilon^2), \tag{4}$$

where $R_0(\xi,\eta)=A(\eta)\cos(\beta\xi)+B(\eta)\sin(\beta\xi)$ and $C^2=A^2+B^2$ is a constant. [Note that in Eq. (4) and in our forthcoming discussion, the small paramater ε has been absorbed back into the constants, so that we need not utilize bars over these quantities.] When $\kappa=\pm 2\beta$, one obtains an extra term due to 2:1 resonance

$$\alpha_R(C)=\alpha(C)\mp\frac{V_0}{4\omega\hbar}+O(\varepsilon^2), \tag{5}$$

where C is defined as before but is no longer constant, and the sign of $V_0/4\omega\hbar$ alternates depending on which equilibrium of the slow dynamics of Eq. (3) one is considering [21].

To examine the band structure of BECs in periodic lattices, we expand Eq. (3) with $V(x)\equiv 0$, $c=0$ in terms of its exact elliptic function solutions, convert to action-angle variables, and apply several canonical transformations to obtain a "resonance Hamiltonian," which we study both analytically and numerically. Using elliptic functions rather than trigonometric functions allows one to analyze $2n$:1 subharmonic resonances with a leading-order perturbation expansion [21,28]. We focus here on the case $g>0$, $\omega>0$. In Reference [21], we also discuss the implication of the work of Zounes and Rand [28] for the case $g<0$, $\omega>0$ and briefly consider the technically more complicated case $g<0$, $\omega<0$. Refs. [15–17] concentrated on numerical studies of band structure. In contrast, we employ Hamiltonian perturbation theory and study the band structure of BECs in periodic potentials both analytically and numerically.

Let $\xi_0=\pi/(2\kappa)$ and $V_1(x)\equiv 0$, so that $V(x)=V_0\cos(\kappa x)$. Equation (3) is then written $R''+\delta R+\alpha R^3+\epsilon R\cos(\kappa x)=0$, where $\delta=2m\omega/\hbar>0$, $\alpha=-2mg/\hbar^2<0$, and $\epsilon=-(2m/\hbar^2)V_0$. (Note that the perturbation parameter

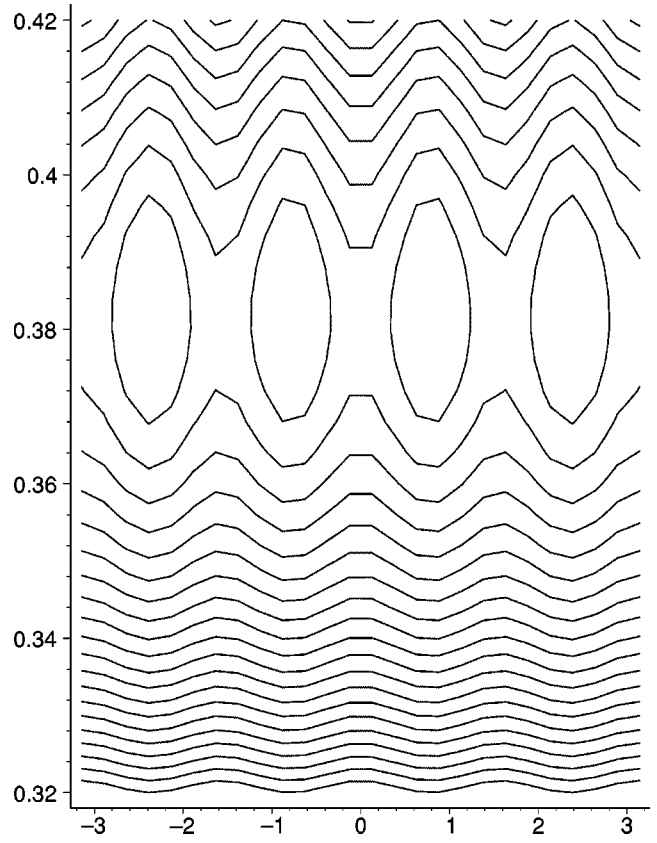

FIG. 3. Resonance Hamiltonian K_2 for $\kappa=2.5$, $\delta=1$, and $\epsilon=0.01$. The vertical axis is in units of action Y, and the horizontal axis is in units of $\xi/J'(Y)$. As discussed in the text, these quantities are scaled and physically unitless.

ϵ is not the same as the parameter ε employed earlier.) When $V_0=0$, one obtains the exact elliptic function solution

$$R=\mu\rho\ \mathrm{cn}(u,k), \tag{6}$$

where $u=u_1x+u_0$, $u_1^2=\delta+\alpha\rho^2$, $k^2=(\alpha\rho^2)/(2[\delta+\alpha\rho^2])$, $u_1\geqslant 0$, $\rho\geqslant 0$, $k^2\in\mathbb{R}$, and $\mu\in\{-1,1\}$. The initial condition parameter u_0 can be set to 0 without loss of generality. We consider $u_1\in\mathbb{R}$ in order to study periodic solutions inside the separatrix (depicted in Fig. 1). One need not retain the parameter μ to do this, so we set it to unity. Because $k^2\in[-\infty,0]$, we utilized the reciprocal complementary modulus transformation in deriving Eq. (6) [29–31,21]. Defining $\chi=\sqrt{\delta}x$ and $r=\sqrt{-\delta/\alpha}R$ and denoting $'\equiv d/d\chi$, the equations of motion take the form

$$r''+r-r^3+\epsilon\delta^{-1}\cos(\kappa\delta^{-1/2}\chi)r=0, \tag{7}$$

with the corresponding Hamiltonian (using $s\equiv r'$)

$$H(r,s,\chi)=\frac{1}{2}s^2+\frac{1}{2}r^2-\frac{1}{4}r^4+\frac{\epsilon}{2\delta}r^2\cos\left(\frac{\kappa}{\sqrt{\delta}}\chi\right). \tag{8}$$

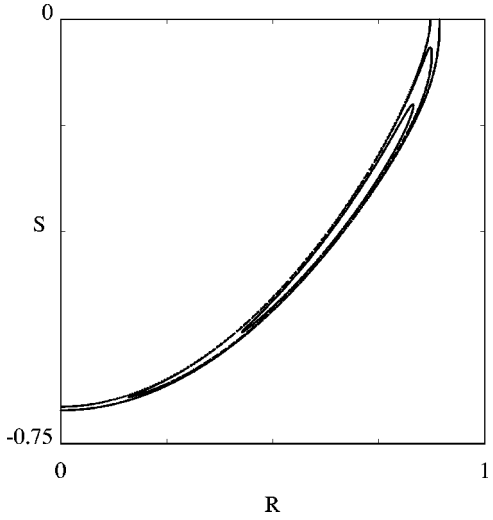

FIG. 4. Lower right corner of a Poincaré section for $\kappa=2.5$, $\delta=1$, and $\epsilon=0.01$. Note that there is no 2:1 resonance band for this choice of (κ,δ). The 4:1 resonance is depicted. (Three additional copies of this structure appear in the Poincaré section.) Recall that the scaled quantities R and S are unitless.

The frequency of a given periodic orbit is $\Omega(k)=\pi\sqrt{1-\rho^2}/[2K(k)]$, where $K(k)$ is the complete elliptic integral of the first kind [32]. One thereby obtains the action [33–36]

$$J=\frac{4\sqrt{1-\rho^2}}{3\pi}\left[E(k)-\left(1-\frac{\rho^2}{2}\right)K(k)\right], \tag{9}$$

where $E(k)$ is the complete elliptic integral of the second kind, and the conjugate angle $\Phi\equiv\Phi(0)+\Omega(k)\chi$. The frequency $\Omega(k)$ decreases monotonically as k^2 goes from $-\infty$ to 0 [as one goes from the separatrix to (0,0)].

After applying several near-identity canonical transformations and expanding elliptic functions in Fourier series [21], one obtains an autonomous resonance Hamiltonian $K_n(Y,\xi)$ (in action-angle coordinates) for the $2n$:1 resonance band,

$$K_n=Y-Y^2-\frac{\kappa J(Y)}{2n\sqrt{\delta}}+\frac{\epsilon}{2\delta}Y\mathcal{B}_n(Y)\cos\left(\frac{2n\xi}{J'(Y)}\right), \tag{10}$$

where $\mathcal{B}_n$ are obtained from Fourier coefficients [21,28]. The band associated with $2n$:1 subharmonic spatial resonances is present when $\kappa/\sqrt{\delta}\leqslant 2n$.

To obtain an analytical description of these resonance bands, we note that such bands emerge from the action $Y=Y_n$, the location of the nth resonance torus in phase space, which is determined by $\kappa/\sqrt{\delta}=2n\Omega(Y_n)$. The saddles and centers of this resonance band are given, respectively, by $Y_s=Y_n-|\Delta Y|$ and $Y_c=Y_n+|\Delta Y|$,

$$\Delta Y=\mp\frac{\epsilon}{2\delta}\left[\frac{\mathcal{B}_n(Y_n)+Y_n\mathcal{B}_n'(Y_n)}{\Omega(Y_n)\sqrt{1-2Y_n}\tilde{K}'(Y_n)-1}\right], \tag{11}$$

where $\tilde{K}'(Y) \equiv 2K'(k(Y))/\pi$, $K'(k) \equiv K(\sqrt{1-k^2})$, $\Delta Y > 0$ when n is even, and $\Delta Y < 0$ when n is odd. The width of resonance bands is

$$W = 2\left| \epsilon \frac{Y_n \mathcal{B}_n(Y_n)}{\delta\left(1 + \frac{\kappa}{2n\sqrt{\delta}} J''(Y_n)\right)} \right|^{1/2}. \tag{12}$$

We compare our analytical results with numerical simulations in (R,S) coordinates with $\alpha = -1$, $m = 1/2$, and $\hbar = 1$. For example, when $\kappa = 2.5$ and $\delta = 1$, the 4:1 resonances are the lowest-order resonances present. The resonance Hamiltonian K_2 is depicted in Fig. 3 for $\epsilon = 0.01$, and the corresponding Poincaré section is shown in Fig. 4. From (10), one predicts that the R-axis saddles are located at $(R,S) = (\pm 0.86364, 0)$, which is rather close to the true value of about $(\pm 0.88, 0)$. The S-axis saddles are predicted to occur at $(R,S) = (0, \pm 0.68389)$, whereas the true value is about $(0, \pm 0.687)$. Numerous other examples are studied in Ref. [21].

At the center of the KAM islands, we observe 'period-multiplied' states. When $n = 1$, these correspond to period-doubled states in ψ [18].

We note, finally, that to analyze three-body interactions (which is necessary, for example, to examine Feshbach resonances [37]), one has to take dissipative effects into account [7,38]. In the present paper, we studied only two-body interactions.

In sum, we employed Lindstedt's method and multiple scale analysis to establish wave number-intensity relations for MAWs of BECs in periodic lattices. With this approach, we studied 2:1 spatial resonances and illustrated the utility of phase space analysis and perturbation theory for the study of band structure as well as the structure of modulated amplitude waves in BECs. Using a more technically demanding perturbative approach relying on the elliptic function structure of solutions of the integrable GP yields the $2n$:1 spatial resonances (band structure) of MAWs, which we studied in considerable detail both analytically and numerically.

Valuable conversations with Eric Braaten, Michael Chapman, Mark Edwards, Nicolas Garnier, Brian Kennedy, Panos Kevrekidis, Yueheng Lan, Boris Malomed, Igor Mezić, Peter Mucha, and Dan Stamper-Kurn are gratefully acknowledged. We are especially grateful to Jared Bronski, Richard Rand, and Li You for several extensive discourses.

[1] C.J. Pethick and H. Smith, *Bose-Einstein Condensation in Dilute Gases* (Cambridge University Press, Cambridge, 2002).
[2] F. Dalfovo *et al.*, Rev. Mod. Phys. **71**, 463 (1999).
[3] W. Ketterle, Phys. Today **52**(12), 30 (1999).
[4] K. Burnett *et al.*, Phys. Today **52**(12), 37 (1999).
[5] M.H. Anderson *et al.*, Science **269**, 198 (1995).
[6] K.B. Davis *et al.*, Phys. Rev. Lett. **75**, 3969 (1995).
[7] T. Köhler, Phys. Rev. Lett. **89**, 210404 (2002).
[8] J.C. Bronski *et al.*, Phys. Rev. Lett. **86**, 1402 (2001).
[9] J.C. Bronski *et al.*, Phys. Rev. E **63**, 036612 (2001).
[10] J.C. Bronski *et al.*, Phys. Rev. E **64**, 056615 (2001).
[11] D.F. Lawden, *Elliptic Functions and Applications*, Applied Mathematical Sciences Vol. 80 (Springer-Verlag, New York, NY, 1989).
[12] R.H. Rand, *Topics in Nonlinear Dynamics with Computer Algebra*, Computation in Education: Mathematics, Science and Engineering Vol. 1 (Gordon and Breach Science Publishers, New York, 1994).
[13] R.H. Rand, a free online book available at *http://www.tam.cornell.edu/randdocs/nlvibe45.pdf*
[14] N.W. Ashcroft and N.D. Mermin, *Solid State Physics* (Brooks/Cole, Australia, 1976).
[15] P.J.Y. Louis *et al.*, Phys. Rev. A **67**, 013602 (2003).
[16] K. Berg-Sørensen *et al.*, Phys. Rev. A **58**, 1480 (1998).
[17] D.-I. Choi and Q. Niu, Phys. Rev. Lett. **82**, 2022 (1999).
[18] M. Machholm *et al.*, Phys. Rev. A (to be published), e-print cond-mat/0307183v1.
[19] F.S. Cataliotti *et al.*, New J. Phys. **5**, 71.1 (2003).
[20] D.G. Fried *et al.*, Phys. Rev. Lett. **81**, 3811 (1998).
[21] M.A. Porter P. Cvitanović, Chaos (to be published), e-print nlin.CD/0308024.
[22] B. Deconinck *et al.*, J. Nonlinear Sci. **12**, 169 (2002).
[23] R. Carretero-González *et al.*, Phys. Rev. A **66**, 033610 (2002).
[24] S. Burger *et al.*, Phys. Rev. Lett. **86**, 4447 (2001).
[25] E.W. Hagley *et al.*, Science **283**, 1706 (1999).
[26] B.P. Anderson and M.A. Kasevich, Science **282**, 1686 (1998).
[27] B.A. Malomed *et al.*, J. Opt. Soc. Am. B **16**, 1197 (1999).
[28] R.S. Zounes *et al.*, Int. J. Non-Linear Mech. **37**, 43 (2002).
[29] V.T. Coppola *et al.*, Nonlinear Dyn. **1**, 401 (1990).
[30] V.T. Coppola, Ph.D. thesis, Cornell University, 1989.
[31] *Handbook of Mathematical Functions With Formulas, Graphs, and Mathematical Tables*, edited by M. Abramowitz and I. Stegun, Applied Mathematics Series Vol.55 (National Bureau of Standards, Washington, D.C., 1964).
[32] E.T. Whittaker and G.N. Watson, *A Course of Modern Analysis*, 4th ed. (Cambridge University Press, Cambridge, 1927).
[33] H. Goldstein, *Classical Mechanics*, 2nd ed. (Addison-Wesley, Reading, MA, 1980).
[34] J. Guckenheimer and P. Holmes, *Nonlinear Oscillations, Dynamical Systems, and Bifurcations of Vector Fields*, Applied Mathematical Sciences Vol. 42 (Springer-Verlag, New York, NY 1983).
[35] S. Wiggins, *Introduction to Applied Nonlinear Dynamical Systems and Chaos*, Texts in Applied Mathematics Vol. 42 (Springer-Verlag, New York, 1990).
[36] A.J. Lichtenberg and M.A. Lieberman, *Regular and Chaotic Dynamics*, 2nd ed., Applied Mathematical Sciences Vol. 38 (Springer-Verlag, New York, NY 1992).
[37] E.A. Donley *et al.*, Nature (London) **412**, 295 (2001).
[38] J.L. Roberts *et al.*, Phys. Rev. Lett. **86**, 4211 (2001).